

A structural model of the anaphase promoting complex co-activator (Cdh1) and in silico design of inhibitory compounds

H. Rahimi¹, B. Negahdari², M.A. Shokrgozar³, A. Madadkar-Sobhani^{4,5}, R. Mahdian¹, A. Foroumadi⁶, M. Kafshdouzi Amin⁷ and M. Karimipoor^{1,*}

¹Department of Molecular Medicine, Biotechnology Research Center, Pasteur Institute of Iran, Tehran, I.R. Iran.

²Department of Medical Biotechnology, Advanced Medical Science School, Tehran University of Medical Sciences, Tehran, I.R. Iran.

³National Cell Bank of Iran, Pasteur Institute of Iran, Tehran, I.R. Iran.

⁴Life Sciences Department, Barcelona Supercomputing Center (BSC), Barcelona 08034, Spain.

⁵Department of Bioinformatics, Institute of Biophysics and Biochemistry (IBB), University of Tehran, Tehran, I.R. Iran.

⁶Faculty of Pharmacy and Pharmaceutical Sciences Research Center, Tehran University of Medical Sciences, Tehran, I.R. Iran.

⁷Faculty of Paramedical Sciences, Qazvin University of Medical Sciences, Qazvin, I.R. Iran.

Abstract

Anaphase promoting complex (APC) controls cell cycle and chromosome segregation. The APC activation occurs after binding of co-activators, cdh1 and cdc20. Cdh1 plays a role in cancer pathogenesis and is known as a potential drug target. The main aim of this study was prediction of 3D structure of cdh1 and designing the inhibitory compounds based on the structural model. First, 3D structure of cdh1 was predicted by means of homology modelling and molecular dynamics tools, MODELLER and Gromacs package, respectively. Then, inhibitory compounds were designed using virtual screening and molecular docking by means AutoDock package. The overall structure of cdh1 is propeller like and each DW40 repeat contains four anti-parallel beta-sheets. Moreover, binding pocket of the inhibitory compounds was determined. The results might be helpful in finding a suitable cdh1 inhibitor for the treatment of cancer.

Keywords: Cdh1; Cancer; Homology modeling; Virtual screening and docking

INTRODUCTION

Approximately 80% of the cellular proteins are dependent on proteasomes for their turnover (1). In cell cycle, this process was controlled by the anaphase promoting complex (APC) and the SKP1-CUL1-F-box protein (SCF). The APC has two active forms namely APC^{cdc20} and APC^{cdh1} whose functions are divided into two groups: cell-cycle dependant and non-mitotic functions (2). APC^{cdc20} is active during the M phase of the cell cycle, while APC^{cdh1} regulates the mitotic exit and the G1 phase as well as cell entrance to the S-phase by recognition of the forkhead box M1 transcription factor (foxM1) and its proteolysis (3-4). In addition, in quiescent cells, APC^{cdh1} is constantly active, resulting in the degradation of Geminin, cdt1 and Cdc6, parts

of the pre-replication complex, that prevents DNA replication (5-6). Inhibition of cdh1 could arrest the cell cycle in the end of M and G1 phase (7). It has recently been shown that an inhibitory system of the APC/C^{cdc20} and APC/C^{cdh1} is critical for the accurate chromosome segregation in the presence of unsatisfied kinetochore-microtubule attachments (8). Several studies have been carried out on the functions of APC in the nervous system. In brain, APC/C^{cdh1} plays a role in the stability of the glycolysis/pentose phosphate pathway by degrading the 6-phosphofructo-2-kinase/fructose-2,6-bisphosphatase-3 (PFKFB3) (9). This 'metabolic program' has enormous impact on neuronal survival (10). Another non-mitotic function of the Cdh1 is related to the control of mitochondrial metabolism, dynamics, and biogenesis which coordinates

*Corresponding author: M. Karimipoor
Tel: 0098 9122806133, Fax: 00982166480780
Email: mortezakarimi@yahoo.com

the cell proliferation with activation of the mitochondrial metabolic machinery (11). Therefore, study of the APC can trigger the development of a novel treatment of neurodegenerative disorders.

The APC will be active after binding to its co-activators Cdh1 and Cdc20 proteins known as WD40 activators (12-13). The co-activators bind to the C-terminal TPR motifs of APC3 and APC8 through the IR domain in the C-terminal region (14-16). Although the IR motif of Cdh1 is bound to TPR groove of the APC3, C-box interacts with other regions (15). Photo-crosslink and a site-directed mutagenesis study of human Cdh1 binding to APC3 have shown that an amino acid near the N-terminal side of C-box (Ser-51), IR tail in the C-terminal (Phe-489) and conserved residues in the WD40 domain (Ser-400 and Phe-444) of Cdh1 could directly bind to APC3. The co-activator binding to the APC is associated with some conformational changes because in vitro experiments on *Xenopus* egg extract showed that Nek2A (bind to APC without any activator) can be ubiquitinated only in the presence of the C-box region of the co-activator (17). This hypothesis is also supported by the conformational changes in Cryo-EM map of APC^{Cdh1} (18).

It has been shown that cdh1 over-expression is associated with pathogenesis of different types of cancers (19-21). Disruption of the APC^{Cdh1-Skp2} cascade in breast cancer is correlated with aggressive clinical behaviour and poor prognosis (22). Genomic instability and tumor suppression stem from the over-expression of the APC co-activator, Cdh1 (23). Since, the mutant embryos died in the early stage of life due to a defect in the endo-reduplication and structural chromosomal aberrations in Cdh1 was considered as a haplo-insufficient tumor suppressor (23). The occurrence of mitotic slippage in the presence of nocodazole, a dilemma for cancer treatment, has been related to the cdh1. Thus, the prevention of such an event together with the APC/C-Cdh1 inhibition might be a useful approach in cancer therapy with mitotic spindle poisons (8,24). The over-expression of APC substrates (securin, Plk1, Skp2, and aurora A), inhibitor (Emi1) and activator (Cdh1) has been revealed by a tissue

microarray analysis on 1600 cancer tissues (20). Moreover, the uniformity of Cdh1 over-expression in malignant tumors would be valuable evidence of the role of Cdh1 in cancer pathogenesis (20). Therefore, the aims of this study were a three-dimensional structure prediction of the DW40 region of cdh1 and design the inhibitory compounds based on structural information. The results showed that cdh1 is composed of many beta-sheets which circle around a central axis. Furthermore, the designed compounds had a high affinity to cdh1 as a drug target. The results are useful for targeting cdh1 as a target in cancer treatment.

MATERIALS AND METHODS

Structure prediction

Homology modeling (HM) protocol was used for prediction of the WD40 domain of cdh1. HM was performed using the MODELLER 9.11 package (25). This software works based on satisfaction of the spatial restraints method, which uses geometrical information (protein data bank, PDB file) to make a probability density function for the position of each atom in the protein (26). Structure prediction process involves steps including fold assignment, target-template alignment, model building, and model evaluation (25). Sequence-structure alignment against PDB database was carried out using BLAST toolkit (27) to find homolog structures as a template in HM. Ten-thousands models were generated and the best model was selected according to the DOPE score (25).

Molecular dynamics simulation

The best model was refined with molecular dynamic (MD) simulation in Gromacs 4.5.4 (28). Force field parameter was the Amber99SB-ILDN force field (29). TIP3P Water model was embedded to the box as solvent (30). The system was neutralized by adding Na and Cl at concentration of 0.15 M, similar to the cell environment. In the position-restrained step, all hydrogen atoms were allowed to relax with the fixed heavy atoms for 50 pico seconds (ps) with step size of 2 femto seconds (fs). This time is the time for making and disruption of the smallest bound,

hydrogen bound, in biological system. All bonds were constrained using the linear constraint solver (LINCS) algorithm (31). A smooth particle mesh Ewald (PME) method was applied for electrostatics and van der Waals (VDW) interactions with the cutoff of 1.4 nm (32). PME was used to calculate the electrostatic interactions with grid spacing of 0.16 nm. The final step of MD simulations was performed with the time step of 2.0 fs for 10 nano second (ns). Energy analysis (temperature, pressure, potential energy, and kinetic energy) and the structure convergence were performed via root mean square deviation (RMSD) against the starting structure and the average structure was investigated. Radius of gyration was calculated to study the global structure in each time. This structure was validated by study of the torsion angles of the protein backbone (ϕ and ψ) via PROCHECK software, Z-score, verify3D, prosaII score, and molprobit (33-34). Ramachandran (ϕ against ψ) plot showed the secondary structure of amino acid and stereochemical quality of amino acid coordination based on torsion angle.

Virtual screening and molecular docking

In order to find the appropriate molecules for docking, structural similarity search approach was used in the ZINC database (35) against C1C (1-(2-carboxynaphth-1yl)-2-naphthoic acid) as standard compound (36). Similarity index was defined at 50% for finding more compounds and for increasing the accuracy. Moreover, the substructure of the compounds was downloaded in the MOL2 format. Ligand and receptor preparation including hydrogen and charge adding and miss-atoms repairing were conducted using ADT4.2 toolkit (37). Then, the docking was performed using vina-autodock (38). The interacting residue diagram was drawn by LigPlot+ software (39). The bioactivity of designed compounds was calculated by means of MOLINSPIRATION server.

RESULTS

Structure prediction and validation

As mentioned above, the WD40 domain of cdh1 plays a critical role in the substrate

recognition and APC activation. Therefore, a computational method was used for structural prediction and inhibitory compounds designing. Domain analysis by means of InterProScan showed that cdh1 contains five WD40 repeats in tandem manner in the C-terminal region (230-471) (Fig. 1).

The 3D structure of the domain was predicted via crystallography structure of cdc20 (PDB ID: 4GGA) as a template in HM. This structure was found in the sequence-structure alignment by BLAST software against PDB data bank. Since the Cdc20 has WD40 domain and a similar function to the cdh1 in the cell cycle, it would be a suitable template for HM (Identity; 41%, E-value; $1.4e-53$) (Fig. 2). The best model was selected based on the DOPE score among 10,000 generated models in MODELLER software. The overall structure folded into a canonical seven-bladed β propeller in which the length of the blade was raised gradually (Fig. 3A). Each WD40 repeat contains four sheets in anti-parallel orientation apart from the first blade which has three sheets as shown in Fig. 3A. In the repeats, the longest sheet was positioned in the outer wall and the smallest one was in the center of the structure. Such orientation helps to generate a complete circle structure. Each blade is bound to the neighbourhood one via the connection of its smallest sheet (inner) to the longest sheet (outer) of the next blade (Fig. 3B). The structure quality was confirmed by the Ramachandran and RMSD plots (Figs. 4A and B). The RMSD showed that the predicted structure was stable after 4 ns simulation. Statistical analysis of Ramachandran plot illustrated that 91% (243 amino acids) of residues are located in the most favored region, 8.2% (22 amino acids) in additional allowed region and 0.7% (2 residues) in generously allowed region (Fig. 4A). On the other hand, no residues in disallowed region was found. Therefore, the coordination of residues in the predicted model was correct.

Virtual screening and molecular docking

As mentioned above, the APC activation is dependent on the binding of Cdh1 to the APC via the WD40 domain.

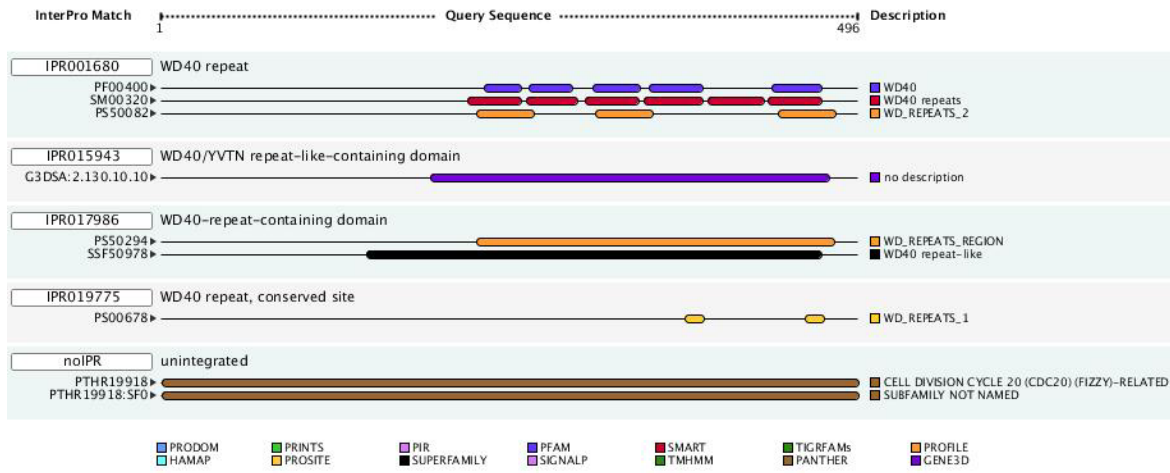


Fig. 1. Pattern of domain distribution in *cdh1*. DW40 repeat domains seen in tandem manner from central until C-terminal region.

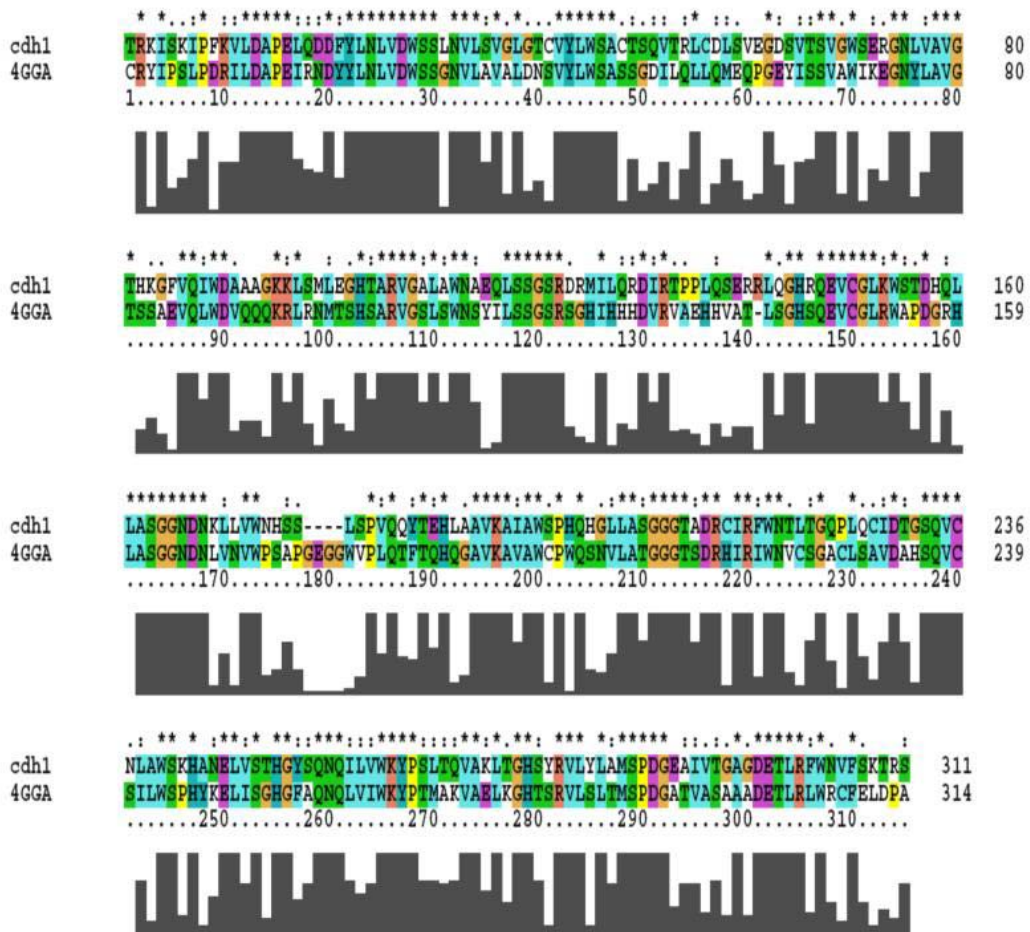


Fig. 2. Sequence-structure alignment of *cdh1* and *cdh20*. Alignment of 4GGA structure, *cdc20*, with *cdh1*. The starfish mark showed conserved residues and similar amino acid is shown by point mark. This alignment used for model building in homology modelling.

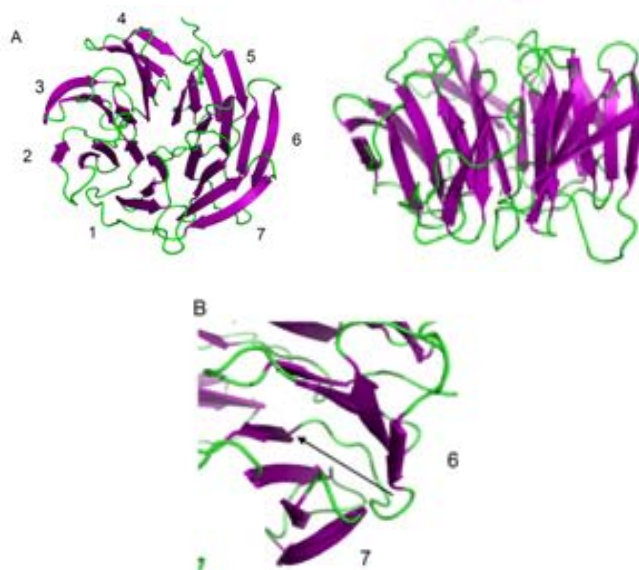


Fig. 3. Cartoon representation of structural model of cdh1. A; Top view showing a front of cdh1 which is composed of seven blades with different lengths around the central axis. The down view showed the edge of the structure which contains many beta-sheets in anti-parallel orientation. B; Binding pattern of DW40 domain to each other in inner to outer mode.

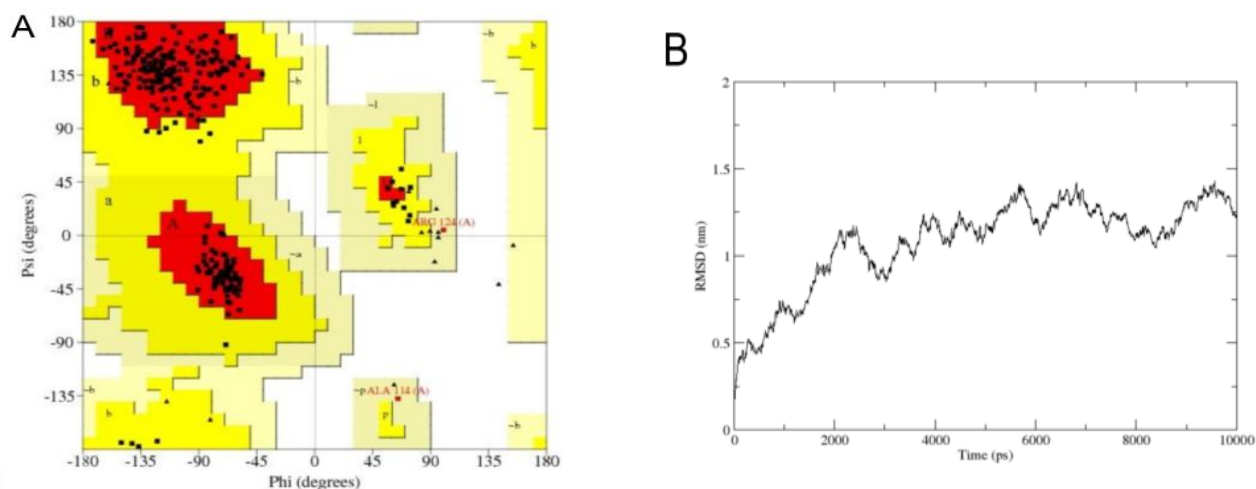


Fig. 4. Structural validation of the cdh1 model. A; In Ramachandran plot all of residues are seen in allowed region B; Root mean square of deviation (RMSD) showed that the cdh1 structure model is energy minimized after 4 ns simulation and had conformational change in each two nano-seconds.

Inhibition of the DW40 domain in yeast causes activity inhibition (36). Therefore, in this study the virtual screening was used to determine a similar compound to C1C (1-(2-carboxynaphth-1yl)-2-naphthoic acid), which is known as WD40 inhibitor (36). By the structural similarity search in the ZINC database against C1C with 50% similarity, 1015 compounds were found. For ligand preparation, the resulted compounds were

introduced to AutoDock 4.2 as input in Mol2 format. Then, molecular docking was performed in Vina-autoDock. After docking, the best four compounds were selected based on the binding score (Table-1 and Fig. 5). Druggability of the selected compounds was done by computation of drug-likeness properties. The drug-likeness and bioactivity scores of the compounds were evaluated with the help of Lipinski's rule, which are

summarized in Table 2 and Table 3, respectively. As shown in Table 4, the binding energy of these compounds is between -8.3 kcal/mol and -7.6 kcal/mol. Binding of the best ligands with Cdh1 is shown in Fig. 6. Among these, the binding pocket of the C compound, which had the highest binding affinity, was visualized in the stick model (Fig. 6B) and a spatial connectivity between the ligand and the

binding pocket residues was observed. The two-dimensional representation of this binding pocket revealed nine van der Waals interactions with Cdh1 (Fig. 6C). In this binding model, aromatic carbon and COO group are involved in interaction. The binding sites of the C compounds were found to be TRP 196, ALA 239, ALA 195, Trp 240, Leu238, Lys153, Thr156, Trp112, and Trp154.

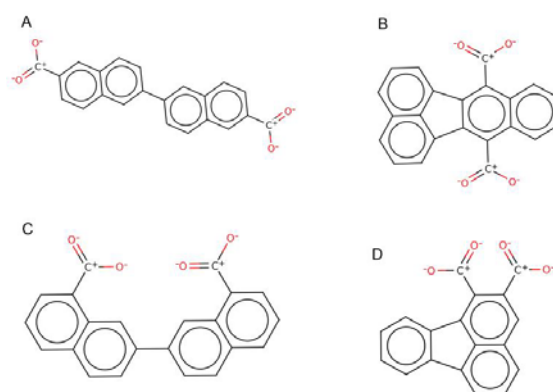


Fig. 5. Two-dimensional representation of the best compounds. A; Bilirubin di-acetyl-?-d-glucuronide (ZINC ID: 65734826), B; Benzo[k]fluoranthene-7,12-dicarboxylic (ZINC ID: 44225038), C; 7-(8-carboxy-2-naphthyl)naphthalene-1-carboxylic (ZINC ID: 59939927) and D; Fluoranthene-1,2-dicarboxylic (ZINC ID: 60162276).

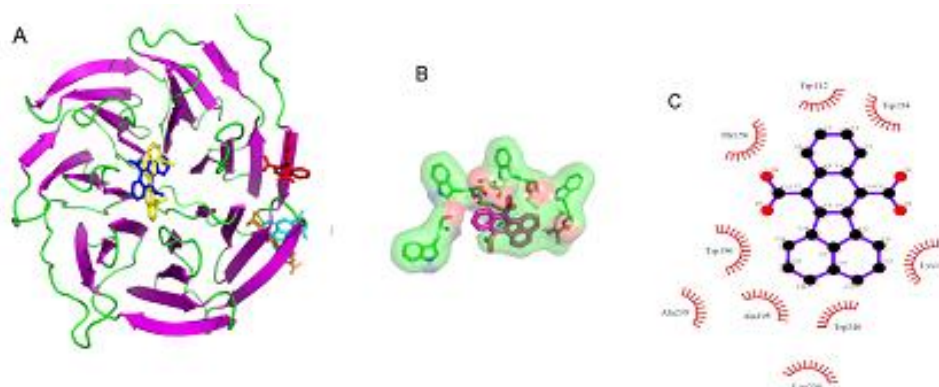


Fig. 6. Binding pocket of cdh1 inhibitors. A; Binding of compounds to chd1 in stick view. C1C and D and A compound bind to same place in edge region but B and C compounds bind to the centres of structure (the C1c, A, B, C and D compounds are shown in red, orange, blue, yellow and cyan colors, respectively). B and C; Binding pattern of C compound as the best ligand in stick and two-dimensional representation.

Table 1. Designed inhibitory compounds for Cdh1 inhibition.

ZINC ID/name here	Smile format	Popular name
ZINC 59939927-(c)	<chem>c1cc2ccc(cc2c(c1)C(=O)[O-])c3ccc4cccc(c4c3)C(=O)[O-]</chem>	7-(8-carboxy-2-naphthyl)naphthalene-1-carboxylic
ZINC 44225038-(b)	<chem>c1ccc2c(c1)c(c-3c(c2C(=O)[O-])c4cccc5c4c3ccc5)C(=O)[O-]</chem>	Benzo[k]fluoranthene-7,12-dicarboxylic
ZINC 65734826(a)	<chem>c1cc(cc2c1cc(cc2)C(=O)[O-])c3ccc4cc(ccc4c3)C(=O)[O-]</chem>	Bilirubin Di-acetyl-?-D-glucuronide
ZINC 60162276-(d)	<chem>c1ccc-2c(c1)-c3cccc4c3c2c(c(c4)C(=O)[O-])C(=O)[O-]</chem>	Fluoranthene-1,2-dicarboxylic

Table 2. Druggability of Cdh1 inhibitory compounds.

Compounds	pH	xlogP	Ap D	P D	H-D	H-A	Net charge	tPSA (Å ²)	MW	R bonds	Heavy atoms
C	7	5.15	13.28	110.24	0	4	-2	80	340.334	3	26
B	7	4.99	13.36	132.05	0	4	-2	80	338.318	2	26
A	7	5.07	13.5	101.15	0	4	-2	80	340.334	3	26
D	7	5.71	1.35	153.96	0	4	-2	80	366.372	4	28

Table 3. Bioactivity of Cdh1 inhibitory compounds.

Compound	GPCR ligand	Ion channel modulator	Kinase inhibitor	Nuclear receptor ligand	Protease inhibitor	Enzyme inhibitor
C	0.1	0.06	0.08	0.22	0.05	0.14
B	0.06	-0.04	-0.17	0.11	-0.08	0.1
A	0.1	0.03	0.1	0.26	0.08	0.15
D	0.03	-0.03	-0.26	0.04	-0.16	0.19

Table 4. Binding energies of the compounds (kcal/mol). For each compounds, different conformation clustered in nine classes based on energy score.

Compounds	Conformational clusters								
	1	2	3	4	5	6	7	8	9
C	-8.3	-8.2	-7.7	-7.6	-7.6	-7.6	-7.6	-7.6	-7.4
B	-8.2	-8.2	-8.2	-8.1	-8.1	-7.8	-7.5	-7.5	-7.5
A	-8.07	-7.4	-7.4	-7.3	-7.3	-7.2	-7.2	-7.2	-7.1
D	-8.1	-7.7	-7.1	-7.0	-7.0	-6.9	-6.9	-6.9	-6.8
C1C	-7.6	-7.4	-7.4	-7.4	-7.1	-7.1	-7.1	-7.0	-7.0

DISCUSSION

The APC, as the largest E3 ligase with 15 subunits, contains RING-Cullin, TPR and DW40 domain (40). The APC activation is dependent on the binding to the DW40 domain of cdh1. The DW40 domain mediates protein-protein interaction (41). Cdh1 via this property could recognize a wide range of substrates and APC subunits (42). In the current study, the structural model of human cdh1 was predicted using homology modelling and molecular dynamics. Then, in order to find the inhibitory compounds for cdh1 inhibition, virtual screening and molecular docking were applied. The results showed that cdh1 structure is composed of seven blades around a circle axis (Fig. 3). Such planar structure could help to recognize substrates with different lengths. In molecular dynamic simulation, after 4 ns, the structure was stable, but, as shown in Fig. 4, there was a repeated conformational change in every two seconds. This was seen in APC10 which is involved in the recognition of the substrate (43). A possible hypothesis would be the acceleration of these subunits binding to the substrates with different conformations.

The overall structure of the WD40 domain is similar to the other WD40 proteins such as Cdc20 and Wdr5 (44-45); however, the blades are greater, the first one is composed of a smaller sheet and the outer sheet is missing (Fig. 3). Furthermore, the size of the central hole is shorter than that of the Cdc20 (45). Although, the human Cdc20 x-ray showed the close orientation of the N-terminal and C-terminal, such a structure was not observed in the present study.

Virtual screening and structure based drug designing (known as rational drug design) were used to design new inhibitors (46-47). There are several examples of approved drugs which are designed by using this strategy. The first example is dorzolamide (trade name Trusopt, (Merck), which is used for glaucoma treatment. The second example, captopril, is a drug that lowers the blood pressure. Enalapril, another effective ACE inhibitor, is a further development of captopril. Thus, this methodology was selected for finding the inhibitory compounds of cdh1. The low concentration (12 μ M) of C1C could inhibit the yeast SCF in tube (36). In this study, the four selected compounds had higher affinity

(>-8) in comparison with C1C (-7.6) (Table 4). It has been shown that *cdh1* inactivation may lead to cell cycle arrest (48). The correlation of over-expression of the APC co-activators (*cdh1* and *cdc20*) with the pathogenesis of different types of cancers was presented by several studies (19-21). Therefore, these compounds are able to inhibit the *cdh1*. Moreover, proteins which contain DW40 domain such as *cdc20* and SCF have a regulatory role in the cell cycle (36). In conclusion, *cdh1* inhibition would be a potential drug target and the designed compounds may be useful for cancer treatment.

CONCLUSION

In this study the structural model of *cdh1* was predicted by means of computational methods. The resulted structure is propeller-like and contains seven blades. Also we designed inhibitory compounds based on structural model. These compounds bound to *Cdh1* in high affinity and carboxylic and aromatic groups are involved in the interaction. Study the effect of designed compounds on cancer cell lines could help to understand the effect of *cdh1* inhibition in cell cycle arrest.

ACKNOWLEDGMENTS

This work was funded by the Ph.D student (Hamzeh Rahimi) grant from Pasteur Institute of Iran.

REFERENCES

1. Heilman DW, Green MR, Teodora JG. The anaphase promoting complex: A critical target for viral proteins and anti-cancer drugs. *Cell Cycle*. 2005;4:560-563.
2. Eguren M, Manchado E, Malumbres M. Non-mitotic functions of the Anaphase-Promoting Complex. *Semin Cell Dev Biol*. 2011;22:572-578.
3. Park HJ, Costa RH, Lau LF, Tyner AL, Raychaudhuri P. Anaphase-promoting complex/cyclosome-Cdh1-mediated proteolysis of the forkhead box M1 transcription factor is critical for regulated entry into S phase. *Mol Cell Biol*. 2008;28:5162-5171.
4. Hyun JP, Costa RH, Lau LF, Tyner AL, Raychaudhuri P. Anaphase-promoting complex/cyclosome-Cdh1-mediated proteolysis of the forkhead box M1 transcription factor is critical for regulated entry into S phase. *Mol Cell Biol*. 2008;28:5162-5171.
5. Clijsters L, Ogink J, Wolthuis R. The spindle checkpoint, APC/C(Cdc20), and APC/C(Cdh1) play distinct roles in connecting mitosis to S phase. *J Cell Biol*. 2013;201:1013-1026.
6. Mailand N, Diffley JFX. CDKs Promote DNA replication origin licensing in human cells by protecting Cdc6 from APC/C-dependent proteolysis. *Cell*. 2005;122:915-926.
7. Horn SR, Thomenius MJ, Johnson ES, Freel CD, Wu JQ, Coloff JL, et al. Regulation of mitochondrial morphology by APC/CCdh1-mediated control of Drp1 stability. *Mol Biol Cell*. 2011;22:1207-1216.
8. Toda K, Naito K, Mase S, Ueno M, Uritani M, Yamamoto A, et al. APC/C-Cdh1-dependent anaphase and telophase progression during mitotic slippage. *Cell Div*. 2012;7:4.
9. Rodriguez-Rodriguez P, Almeida A, Bolanos JP. Brain energy metabolism in glutamate-receptor activation and excitotoxicity: role for APC/C-Cdh1 in the balance glycolysis/pentose phosphate pathway. *Neurochem Int*. 2013;62:750-756.
10. Herrero-Mendez A, Almeida A, Fernandez E, Maestre C, Moncada S, Bolanos JP. The bioenergetic and antioxidant status of neurons is controlled by continuous degradation of a key glycolytic enzyme by APC/C-Cdh1. *Nat Cell Biol*. 2009;11:747-752.
11. Garedew A, Andreassi C, Moncada S. Mitochondrial dynamics, biogenesis, and function are coordinated with the cell cycle by APC/C(CDH1). *Cell Metab*. 2012;15:466-479.
12. Sudo T, Ueno NT, Saya H. Functional analysis of APC-Cdh1. *Methods in molecular biology* (Clifton, NJ). 2004;281:189-198.
13. Skaar JR, Pagano M. Cdh1: A master G0/G1 regulator. *Nature Cell Biology*. 2008;10:755-757.
14. Thornton BR, Ng TM, Matyskiela ME, Carroll CW, Morgan DO, Toczyski DP. An architectural map of the anaphase-promoting complex. *Genes & Development*. 2006;20:449-460.
15. Matyskiela ME, Morgan DO. Analysis of activator-binding sites on the APC/C supports a cooperative substrate-binding mechanism. *Molecular Cell*. 2009;34:68-80.
16. Vodermaier HC, Gieffers C, Maurer-Stroh S, Eisenhaber F, Peters J-M. TPR subunits of the anaphase-promoting complex mediate binding to the activator protein CDH1. *Current biology: CB*. 2003;13:1459-1468.
17. Kimata Y, Baxter JE, Fry AM, Yamano H. A role for the fizzy/Cdc20 family of proteins in activation of the APC/C distinct from substrate recruitment. *Mol Cell*. 2008;32:576-583.
18. Dube P, Herzog F, Gieffers C, Sander B, Riedel D, Muller SA, et al. Localization of the coactivator Cdh1 and the cullin subunit Apc2 in a cryo-electron microscopy model of vertebrate APC/C. *Mol Cell*. 2005;20:867-879.

19. Chang DZ, Ma Y, Ji B, Liu Y, Hwu P, Abbruzzese JL, *et al.* Increased CDC20 expression is associated with pancreatic ductal adenocarcinoma differentiation and progression. *J Hematol Oncol.* 2012;5:15.
20. Lehman NL, Tibshirani R, Hsu JY, Natkunam Y, Harris BT, West RB, *et al.* Oncogenic regulators and substrates of the anaphase promoting complex/cyclosome are frequently overexpressed in malignant tumors. *Am J Clin Pathol.* 2007;170:1793-1805.
21. Mondal G, Sengupta S, Panda CK, Gollin SM, Saunders WS, Roychoudhury S. Overexpression of Cdc20 leads to impairment of the spindle assembly checkpoint and aneuploidization in oral cancer. *Carcinogenesis.* 2007;28:81-92.
22. Fujita T, Liu W, Doihara H, Date H, Wan Y. Dissection of the APCCdh1-Skp2 cascade in breast cancer. *Clin Cancer Res.* 2008;14:1966-1975.
23. Garcia-Higuera I, Machado E, Dubus P, Canamero M, Mendez J, Moreno S, *et al.* Genomic stability and tumour suppression by the APC/C cofactor Cdh1. *Nat Cell Biol.* 2008;10:802-811.
24. Lee J, Kim JA, Margolis RL, Fotadar R. Substrate degradation by the anaphase promoting complex occurs during mitotic slippage. *Cell Cycle.* 2011;9:1792-1801.
25. Eswar N, Webb B, Marti-Renom MA, Madhusudhan MS, Eramian D, Shen MY, *et al.* Comparative protein structure modeling using MODELLER. *Curr Protoc Protein Sci.* 2007 Nov;Chapter 2:Unit 2.9:1-31.
26. Eswar N, Eramian D, Webb B, Shen MY, Sali A. Protein structure modeling with MODELLER. *Methods Mol Biol.* 2008;426:145-159.
27. Park Y, Sheetlin S, Ma N, Madden TL, Spouge JL. New finite-size correction for local alignment score distributions. *BMC Res Notes.* 2012;5:286.
28. Van der Spoel D, Lindahl E, Hess B, Groenhof G, Mark AE, Berendsen HJC. GROMACS: Fast, flexible, and free. *J COMPUT Chem.* 2005;26:1701-1718.
29. Lindorff-Larsen K, Piana S, Palmo K, Maragakis P, Klepeis JL, Dror RO, *et al.* Improved side-chain torsion potentials for the Amber ff99SB protein force field. *Proteins.* 2010 ;78:1950-1958.
30. Jorgensen WL, Chandrasekhar J, Madura JD, Impey RW, Klein ML. Comparison of simple potential functions for simulating liquid water. *J Chem Phys.* 1983;79:926-935.
31. Hess B, Bekker H, Berendsen HJC, Fraaije JGEM. LINCS: A linear constraint solver for molecular simulations. *J Comput Chem.* 1997;18:1463-1472.
32. Merlino A, Mazzarella L, Carannante A, Di Fiore A, Di Donato A, Notomista E, *et al.* The importance of dynamic effects on the enzyme activity: X-ray structure and molecular dynamics of onconase mutants. *J Biol Chem.* 2005;280:17953-17960.
33. Laskowski RA, MacArthur MW, Moss DS, Thornton JM. PROCHECK: a program to check the stereochemical quality of protein structures. *J Appl Crystallogr.* 1993;26:283-291.
34. Luthy R, Bowie JU, Eisenberg D. Assessment of protein models with three-dimensional profiles. *Nature.* 1992;356:83-85.
35. Irwin JJ, Shoichet BK. ZINC--a free database of commercially available compounds for virtual screening. *J Chem Inf Model.* 2005;45:177-182.
36. Orlicky S, Tang X, Neduva V, Elowe N, Brown ED, Sicheri F, *et al.* An allosteric inhibitor of substrate recognition by the SCF(Cdc4) ubiquitin ligase. *Nat Biotechnol.* 2010;28:733-737.
37. Morris GM, Huey R, Lindstrom W, Sanner MF, Belew RK, Goodsell DS, *et al.* AutoDock4 and AutoDockTools4: Automated docking with selective receptor flexibility. *J Comput Chem.* 2009;30:2785-2791.
38. Trott O, Olson AJ. AutoDock Vina: Improving the speed and accuracy of docking with a new scoring function, efficient optimization, and multithreading. *J Comput Chem.* 2010;31:455-461.
39. Laskowski RA, Swindells MB. LigPlot+: multiple ligand-protein interaction diagrams for drug discovery. *J Chem Inf Model.* 2011;51:2778-2786.
40. Herzog F, Primorac I, Dube P, Lenart P, Sander B, Mechtler K, *et al.* Structure of the anaphase-promoting complex/cyclosome interacting with a mitotic checkpoint complex. *Science.* 2009;323:1477-1481.
41. Yu H. Cdc20: A WD40 activator for a cell cycle degradation machine. *Molecular Cell.* 2007;27:3-16.
42. Kraft C, Vodermaier HC, Maurer-Stroh S, Eisenhaber F, Peters J-M. The WD40 propeller domain of Cdh1 functions as a destruction box receptor for APC/C substrates. *Molecular Cell.* 2005;18:543-553.
43. Buschhorn BA, Petzold G, Galova M, Dube P, Kraft C, Herzog F, *et al.* Substrate binding on the APC/C occurs between the coactivator Cdh1 and the processivity factor Doc1. *Nat. Struct. Mol. Biol.* 2011;18(1):6-14.
44. Han Z, Guo L, Wang H, Shen Y, Deng XW, Chai J. Structural basis for the specific recognition of methylated histone H3 lysine 4 by the WD-40 protein WDR5. *Mol Cell.* 2006;22:137-144.
45. Tian W, Li B, Warrington R, Tomchick DR, Yu H, Luo X. Structural analysis of human Cdc20 supports multisite degron recognition by APC/C. *Proc Natl Acad Sci U S A.* 2012;109:18419-18424.
46. Ashari A, Davood A, Y Ebrahimi Nasimi B. Synthesis and docking studies of novel antifungals based on 4-substituted imidazole. *Res Pharm Sci.* 2012;7:S579.
47. Ghadimi AA, Azizian H, Mirahmadi S, A Shafiee M. Synthesis and docking studies of new 4-oxo-1, 3-thiazolidine derivatives as potential anticonvulsant agents. *Res Pharm Sci.* 2012;7:S578.
48. Chen M, Gutierrez GJ, Ronai ZA. The anaphase-promoting complex or cyclosome supports cell survival in response to endoplasmic reticulum stress. *Plos One.* 2012;7:e35520.